A Computationally Efficient Doppler Compensation System for Underwater Acoustic Communications

Bayan S. Sharif, *Member, IEEE*, Jeff Neasham, Oliver R. Hinton, and Alan E. Adams

***Abstract*—A Doppler compensation system is presented which is suitable for high-data-rate acoustic communication between rapidly moving platforms such as autonomous underwater vehicles. The proposed approach provides a generic preprocessor to conventional adaptive receiver structures with only a marginal increase in computational load and hardware cost. The preprocessor employs a novel Doppler estimation technique and efficient sample rate conversion to remove Doppler shift induced by platform velocity and acceleration. Performance predicted by simulation is compared to that of sea trials of a prototype communication system in the North Sea. Successful communication is demonstrated at 16 kbit/s with a transmitting platform moving at up to ± 2.6 m/s.**

***Index Terms*—Acoustic telemetry, carrier phase, linear interpolation, symbol synchronization.**

I. Introduction

IN UNDERWATER acoustic communication, carrier tracking and symbol synchronization are adversely affected by Doppler. The low velocity of acoustic waves (~1500 m/s) and the use of wide-band modulation result in Doppler shifts several orders of magnitude greater than those experienced in EM transmission. Relative motion of the transmitting and receiving elements is usually unavoidable, particularly if either end of the link is deployed by a surface vessel which is subject to the effects of sea currents and/or surface waves. Rapidly moving platforms such as autonomous underwater vehicles (AUV's) present a more serious problem. Compensating for Doppler shifts resulting from relative velocities up to 10 m/s is far beyond the capability of conventional adaptive equalization structures, even with explicit phase tracking loops [1]. This paper presents a novel approach based on a Doppler preprocessing structure, compatible with existing adaptive receiver structures, to deal with these severe Doppler effects.

The relative Doppler shift Δ is defined as the ratio of the source relative velocity (v) to the propagation wave velocity (c). For a single-frequency component ω_n, the Doppler effect can be expressed as a frequency scaling

$$\omega_n' = \omega_n(1+\Delta). \tag{1}$$

This is often used as an approximation for narrow-band signals in which the whole signal spectrum is translated by the same frequency as the carrier. The Doppler shift imposed on the carrier is dealt with by carrier synchronization, which is equivalent to adjusting the local carrier frequency. Conventionally, this is achieved using Mth law carrier recovery and/or a phase-locked loop (PLL) [2], [3].

In wide-band signals, Doppler translates each frequency component by a different amount, and the Doppler effect is more accurately modeled as a complete time scaling (expansion or compression) of the signal waveform

$$r(t) = s((1+\Delta)t) \tag{2}$$

where $s(t)$ and $r(t)$ are the source and Doppler-shifted received signals, respectively. This wide-band model of the Doppler effect is used for underwater acoustic communications where the bandwidth can be as high as an octave (e.g., 10–20-kHz band). In this case, symbol synchronization is of equal importance to carrier synchronization. Furthermore, conventional synchronization techniques, such as PLL's when coupled with equalization, are often unreliable in underwater acoustic communications, mainly due to severe multipath distortion and fading [1]. Also, in the PLL, the error loop filter bandwidth required to track Doppler shifts as high as 1% is very difficult to achieve.

If we now consider a discrete-time sampled source signal $s[nT_s]$, where n is an integer and T_s is the sampling period, then introducing a Doppler shift to the received signal in (2) is equivalent to a scaling of the sampling period (interpolation or decimation)

$$r[nT_s] = s[n(1+\Delta)T_s]. \tag{3}$$

If the amount of Doppler shift (Δ) is known, then the received signal can be compressed/expanded by inverse time scaling to remove both carrier and symbol shift. In a multirate discrete-time processing system, this is equivalent to resampling the bandpass signal by 1+Δ

$$s[nT_s] = r\left[\left(\frac{n}{1+\Delta}\right)T_s\right]. \tag{4}$$

Removal of the fractional Doppler shift Δ from a received signal then corresponds to a scaling of the sampling frequency

$$f_s' = (1+\Delta)f_s. \tag{5}$$

This Doppler compensation approach implies a two-stage process; first the Doppler shift must be estimated from the received signal to obtain the interpolation factor $(1+\Delta)$. An interpolator structure is then used to perform a sampling

Manuscript received October 15, 1998; revised June 22, 1999. This work was supported by the CMPT/EPSRC Managed TUUV Programme (Technology for Unmanned Underwater Vehicles) through a research grant.

The authors are with the Department of Electrical and Electronic Engineering, University of Newcastle, Newcastle upon Tyne, NE1 7RU, U.K.

Publisher Item Identifier S 0364-9059(00)00291-0.

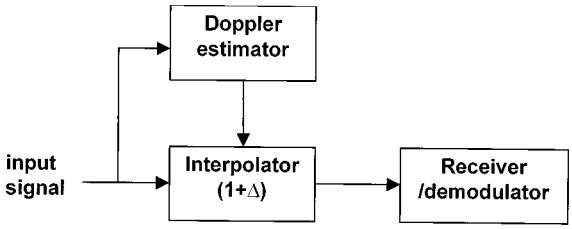

Fig. 1. Doppler estimation/compensation structure.

rate conversion on the incoming samples. The overall system structure is shown in Fig. 1. This approach provides a generic preprocessor that can be used with wide-band receiver structures. The interpolator structure can be used either prior to (bandpass) or after demodulation (baseband). For a complex baseband interpolator structure, the carrier frequency offset must be removed prior to demodulation. Baseband interpolation offers a considerable computational saving for relatively narrow-band signals; however, for underwater acoustic telemetry characterized by wide-band modulation (octave bandwidth), this saving is marginal.

A major design parameter is the degree of accuracy required from the Doppler estimator and interpolator, which is entirely dependent on the amount of residual Doppler that can be tolerated by the receiver/demodulator system. Doppler tolerance of decision feedback equalizers (DFE)'s with an embedded PLL is related to the equalizer's tracking rate, adaptation algorithm, and the phase-tracking loop gain. The DFE is used to track slow channel variations and can only tolerate small levels of Doppler shift whilst maintaining a low mean square error (MSE). At increased levels of Doppler, the DFE is unable to track the fast phase variations, which results in increased MSE, or even equalizer divergence. Previous experimental trials have shown that, for a bandwidth of 10 kHz, such a DFE structure could tolerate fractional Doppler shifts of the order of 10^{-4} [1]. This suggests that the Doppler estimator and interpolator must be accurate to within a factor of 10^{-4} to allow successful communications with such a receiver.

To summarize, the focus of this paper is on the development of a digital signalprocessing (DSP) algorithm to accurately estimate time expansion/compression and then remove the Doppler shift by efficient multirate sampling. The paper is organized as follows. Section II presents Doppler estimation and interpolation methods for Doppler compensation. The effects of platform acceleration are discussed in Section III. Section IV provides details of the sea trial system design, simulation and experimental results. Finally, conclusions are drawn in Section V.

II. Doppler Estimation and Compensation Techniques

A. Ambiguity Function Method

The ambiguity function shows the matched filter response against delay and Doppler shift variations of the incoming signal [4]. For a wide-band continuous time signal, the definition of the ambiguity function is given as

$$\chi_s(\tau, \Delta) = (1+\Delta)\int_{-\infty}^{\infty} s((1+\Delta)t)s(t-\tau)\,dt. \qquad (6)$$

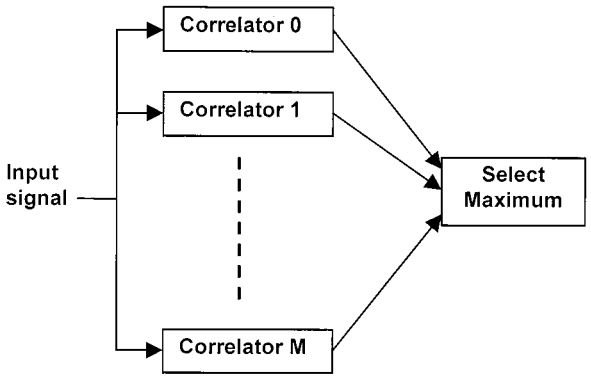

Fig. 2. Multiple correlator structure for Doppler estimation.

If we consider the received signal $r(t)$, then we can define the cross-ambiguity function

$$\chi_{sr}(\tau, \Delta) = (1+\Delta)\int_{-\infty}^{\infty} s((1+\Delta)t)r(t-\tau)\,dt. \qquad (7)$$

To estimate the Doppler shift in $r(t)$, we must search in Δ, with $\tau = 0$ (i.e., with time alignment) to find the maximum magnitude of the cross-ambiguity function $\chi_{sr}(0, \Delta)$:

$$\chi_{sr}(0, \Delta) = (1+\Delta)\int_{-\infty}^{\infty} s((1+\Delta)t)r(t)\,dt. \qquad (8)$$

In practice, we need only search within the anticipated Doppler range, determined from the maximum relative velocity encountered and the wave velocity. This search can be realized as shown in Fig. 2 as a bank of discrete correlators with different Doppler-shifted replicas of the transmitted waveform. Upon synchronization (i.e., when the waveform is fully within the delay lines), the branch yielding the largest correlation peak is then selected to determine the Doppler estimate. The Doppler resolution of this technique depends on: 1) received signal signal-to-noise ratio (SNR); 2) time–bandwidth product of the signal (*BT*); and 3) shape of the signal's ambiguity function. For maximum resolution, a waveform with a narrow peak in the Doppler axis of the ambiguity function is desirable, hence the maximal-length pseudonoise (PN) codes are perhaps most suitable. This method of Doppler estimation has been demonstrated in [5], where a bank of correlators is used to obtain a coarse grain Doppler estimation followed by an interpolator to remove the estimated Doppler shift from the received signal. An equalizer with a PLL is then used to remove any residual Doppler. The range and resolution of the coarse Doppler estimate dictates the number of correlators required. If we consider this approach for our application, for example, where a coarse Doppler resolution of around 0.02% is specified over a Doppler shift range of ±1%, then this suggests that 100 individual correlators are required.

B. Block Doppler Estimation

A more computationally efficient Doppler estimator is proposed in this paper, which can be realized by measuring the duration of a received data packet ($T_{\rm rp}$). Since Doppler manifests itself as packet compression/expansion, it can then be estimated

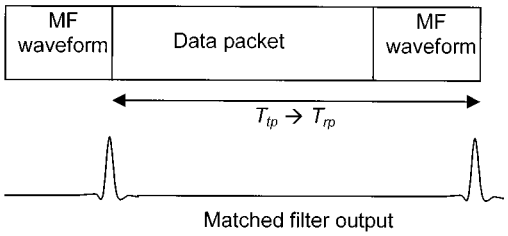

Fig. 3. Packet length measurement using matched filtering.

using *a priori* knowledge of the transmitted data packet duration (T_{tp})

$$\hat{\Delta} = \frac{T_{\rm rp}}{T_{\rm tp}} - 1. \tag{9}$$

The most reliable way to measure the quantity $T_{\rm rp}$ is to interleave data packets with a known waveform, which can be detected using a single correlator. The probability of false detection is minimized by selecting waveforms with a large bandwidth–time product ($BT \geq 100$). This method is illustrated in Fig. 3.

The resolution of the Doppler estimate obtained by this method is dependent upon the bandwidth (B) of the matched filter signal and the length of the transmitted packet ($T_{\rm tp}$). If we consider a nondespersive channel, the time resolution of the matched filter detector is $1/B$, and the Doppler resolution of the estimator is then approximated by

$$\delta\hat{\Delta} \approx \frac{1}{BT_{tp}}. \tag{10}$$

This is a minimum bound, and the estimate will degrade relative to the time dispersion in the channel. Choice of the correlation waveform is governed by the degree of Doppler tolerance required by the receiver. For significant Doppler shifts due to vehicle movement, a mismatch will occur between the received correlation waveform and the single correlator, with a consequent loss of a distinct correlation peak. Therefore, signals with very narrow ambiguity functions in the Doppler axis, such as PN sequences, are ruled out in favor of linear or log frequency-modulated (FM) signals. Such signals are highly Doppler-tolerant due to their wide ambiguity function in the Doppler axis. The expression for a linear frequency-modulated (LFM) signal, also referred to as a "chirp," is given as

$$s(t) = \cos\left(2\pi f_0 t + \pi k t^2\right). \tag{11}$$

The instantaneous frequency is obtained by differentiation

$$f(t) = \frac{1}{2\pi} \cdot \frac{d}{dt}(2\pi f_0 t + \pi k t^2) = f_0 + kt. \tag{12}$$

Hence, the LFM chirp is characterized by its start frequency (f_0), stop frequency (f_1), and time duration (T) as

$$|k| = \frac{|f_1 - f_0|}{T} = \frac{B}{T}. \tag{13}$$

A detailed analysis of the properties of LFM waveforms is found in [4]. We can get a numerical measure of the Doppler tolerance

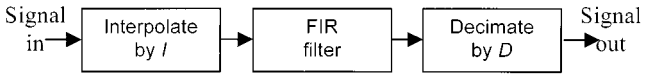

Fig. 4. Sample rate conversion by a rational factor.

of a chirp signal by considering the ambiguity surface. From [4], the half power point of the ambiguity function along the Doppler axis ($\tau = 0$) is approximately given as

$$\Delta_{3\,\rm db} = \frac{1.74}{BT}. \tag{14}$$

For example, with $B = 10$ kHz, $T = 0.01$ s, then $\Delta_{3\,\rm db} = 1.74\%$. This degree of Doppler tolerance is more than adequate for the purposes of our experimental system; however, should a much higher *BT* product be required, then Doppler-invariant (logarithmic) chirps must be used [4]. For an LFM signal, the main ridge of the ambiguity function extends along the correlation delay axis (τ) as a function of Doppler shift. This is derived from [6] as

$$\tau(\Delta) = \frac{T}{B}\frac{\Delta}{(1-\Delta)}\left[\frac{f_{\rm min}}{1-\Delta} - \frac{\Delta f_{\rm max}}{1+\Delta}\right]. \tag{15}$$

For realistic levels of Doppler ($v < 15$ m/s), this delay in the main ridge varies almost linearly with Doppler. Furthermore, if the relative velocity between the source and receiver were constant (i.e., zero acceleration) over the duration of the packet, then the correlation peak at both ends of the packet will undergo the same time offset, and no error in Doppler estimation will result.

C. Interpolation Methods

Sample rate conversion is a demanding task, particularly when a high degree of accuracy is required (~0.02%) for small Doppler shifts (~1%). The usual approach is to convert the sampling rate by a rational number I/D, where D and I are relatively prime integers. This approach is shown in Fig. 4 and can be implemented using polyphase filters [7]. However, in this application, the number of subfilters are very large, and the resulting computational load in updating such a large filter bank each time the Doppler estimate changes is considerable. Alternatively, a more computationally efficient method such as linear interpolation can be used to calculate each new sample. Linear interpolation can be performed either on the real bandpass signal or the complex baseband signal after carrier phase correction. In narrow-band communication systems (i.e., $f_c \gg B$), considerable saving in computations is possible by interpolating the baseband signal. However, in this wideband application ($f_c = 1.5B$), the computational saving is very small and interpolating the bandpass is more convenient. The sampling rate for the interpolator f_s should be considerably faster than the Nyquist rate in order to minimize the error between the straight-line approximation and the analog waveform. The interpolator's performance is measured by the signal-to-distortion ratio (SDR) at the output [7], which for a given signal frequency (f) is approximated as

$$\text{SDR(dB)} \approx 40\,\log_{10}\left(\frac{2f_s}{f}\right). \tag{16}$$

The SDR must not be lower than the maximum SNR anticipated at the receiver; otherwise, a penalty in receiver performance will result.

III. Acceleration Effects

Thus far, we have only considered Doppler shift under the assumption of constant velocity. To take into account the effect of constant acceleration (α) either by the source or receiver platform, the expression for the time-varying Doppler shift is given as

$$\Delta_t = \Delta_0 + \frac{\alpha t}{c} \tag{17}$$

where Δ_0 is the Doppler shift due to the initial platform velocity. In order to investigate the effect of this Doppler shift on the estimation/compensation process, we need to consider the techniques discussed in Section III, viz. PN and chirp signals. A PN sequence having a narrow ambiguity function can lead to mismatch problems if the search is done only in velocity. A two-dimensional search in velocity and acceleration is a possible solution, albeit at the expense of a significant increase in computation load.

Using the chirp-interleaved block estimation method, accounting for acceleration is a manageable task subject to a few extra realistic constraints on the system parameters. We can justifiably assume that the change in velocity within a chirp duration is much smaller in magnitude than the maximum platform velocity. This implies that the extra mismatch introduced has an insignificant effect on the chirp correlation peak. However, a more significant consideration is acceleration over the whole transmission packet. This has a twofold effect on the Doppler estimation error. First, if we consider that the start and end chirps undergo different Doppler shifts, this results in different time lags of the two main correlation peaks (15), and consequently adds an error to the Doppler estimate. To estimate this error, we assume without loss of generality that the initial velocity is zero. Then, from (15) and (17), for $\Delta \ll 1$ and octave bandwidth ($B = f_{\min} = 0.5 f_{\max}$), the error is approximated as

$$\varepsilon'_{\Delta} \approx \frac{\alpha T}{c}. \tag{18}$$

This contribution of this error to Doppler estimation is unrelated to the data packet length and is usually very small for realistic acceleration levels (~1 m/s2). The other more significant effect of acceleration over the packet length is related to the residual Doppler tolerable by conventional adaptive equalization and phase-tracking structures. Under the assumption of constant acceleration, block Doppler estimation yields an estimate corresponding to the mean velocity, i.e., at the mid-point of the packet duration, and hence, the max residual Doppler at the packet ends is given as

$$\max\left(\Delta_{\text{residual}}\right) = \pm\frac{\alpha T_{tp}}{2c}. \tag{19}$$

This suggests that, for high acceleration, mitigating residual Doppler entails reducing the packet length in order to estimate the Doppler shift more frequently. This approach infers an approximation to a constant velocity over the packet, by fitting a straight-line approximation to the quadratic displacement curve shown in Fig. 5. However, significant reduction of the data packet length ultimately reduces bandwidth efficiency by a factor ($1 - T/T_{\text{tp}}$). A more robust technique, particularly useful for platforms with very high acceleration, uses the Doppler estimate for several successive packets to estimate acceleration (or higher order components). A time-varying interpolation factor can then be used to give a more accurate Doppler compensation.

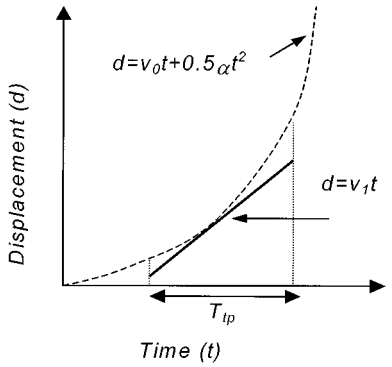

Fig. 5. Constant velocity approximation to accelerating motion.

TABLE I
Experimental System Specification

Frequency band	10-20kHz
Modulation format	Coherent QPSK @ 10kBaud
Receiver type	LMS jointly adaptive beamformer & DFE [1]
Doppler Tolerance	~0.02% (uncompensated)
Baseband sampling	I-Q sampling at 20kHz ($T/2$ spacing)
Training data	511 symbol PN Sequence
SNR	~20dB
Max velocity	±3m/s
Max Acceleration	±1m/s^2 typical
Data throughput	~80% (16kbits/s)

IV. System Design, Simulation, and Experimental Results

A. System Design Parameters

The experimental setup for real-time implementation of the Doppler-tolerant receiver structure is shown in Table I.

1) Interpolator Input Sampling Rate: To determine the interpolator's sampling rate, we must first establish what level of spectral distortion is acceptable. From Table I, for a received SNR of ~20 dB and also considering some residual multipath, the overall signal to interference + noise ratio (SINR) at the receiver output will rarely exceed ~15 dB. Hence, if the interpolator's SDR is >20 dB then no significant penalty in receiver

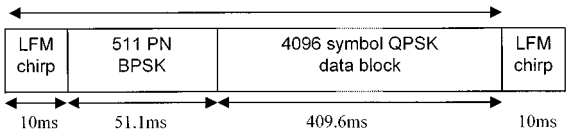

Fig. 6. Transmitted packet structure.

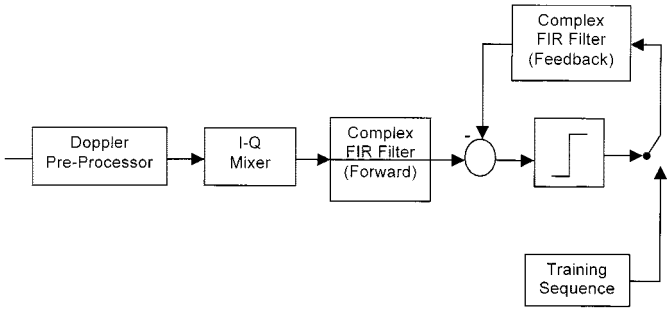

Fig. 7. Block diagram of the overall receiver structure.

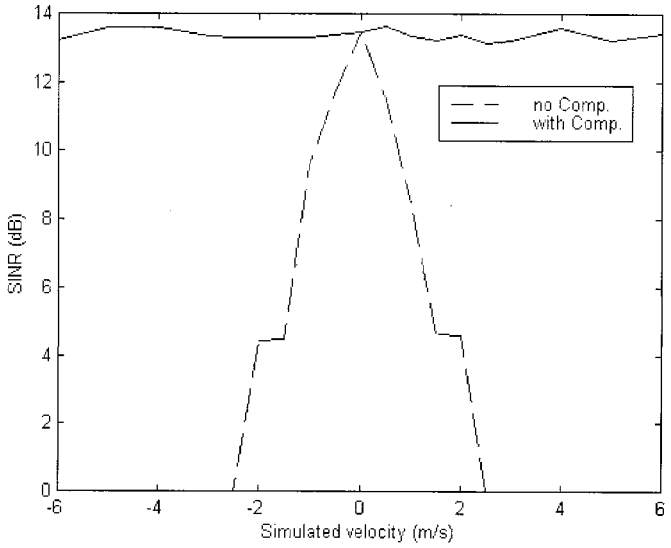

Fig. 8. Output SINR versus transmitter velocity for simulated signals with zero acceleration.

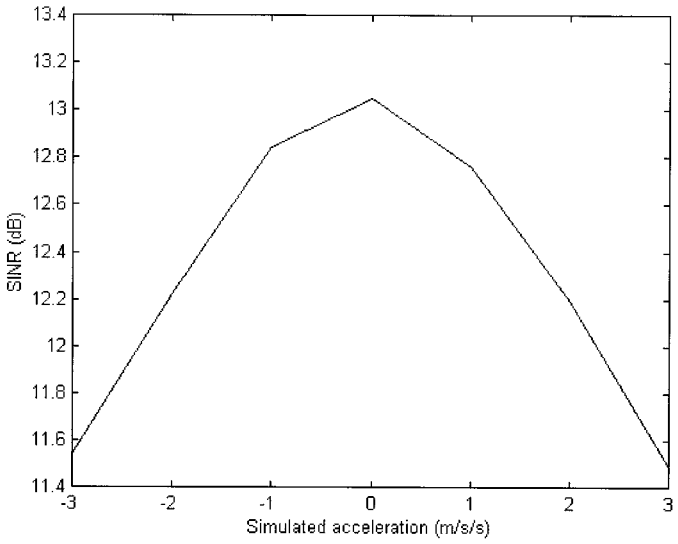

Fig. 9. Output SINR versus transmitter acceleration for simulated signals with zero starting velocity.

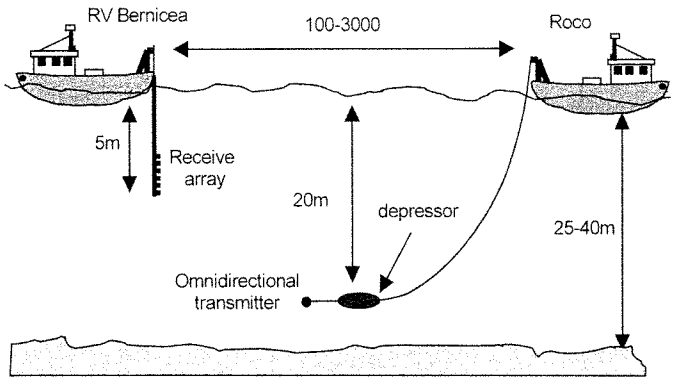

Fig. 10. Experimental configuration for the sea trial.

performance should result. Using (16), we find that a sampling rate of 100 kHz gives an expected SDR of 20.9 dB for a center frequency of 15 kHz, which is sufficient for this application.

2) Parameters of Chirp Waveform: The bandwidth of the chirp signal is chosen to span the available channel bandwidth (10 kHz) in order to minimize the length of the chirp ($T \ll T_{\rm tp}$) for a given *BT* product. Choosing the *BT* product is governed by the amount of matched filtering gain required to achieve a reliable detection threshold. A gain of 20 dB ($BT = 100$) was empirically determined to be sufficient, and accordingly the chirp signal is a 10-ms 10–20-kHz frequency sweep. From (14), we find that the half power point of the ambiguity surface of this waveform occurs at a Doppler shift of approximately 1.74%. Hence, the detection threshold should not vary significantly over the $\pm 1\%$ range required for the application investigated.

3) Packet Structure and Dimensions: The packet structure used in the simulation and the experiment is shown in Fig. 6. The system bandwidth of 10 kHz (10–20 kHz) is swept by a 10-ms LFM chirp which is inserted at the start and end of each phase-shift keying (PSK) signal block. The signal block comprises an equalizer training sequence of 511 binary PSK (BPSK) symbols and a quadrature PSK (QPSK) data block (both at 10 kbaud symbol rate). The length of this QPSK block is the main variable parameter to control the performance of the Doppler compensation system. To determine the required packet length ($T_{\rm tp}$), we must first consider the required Doppler resolution. From Table I, the maximum residual Doppler that the adaptive receiver structure can tolerate is given as 0.02%. To obtain this Doppler resolution, (14) suggests a block length of ~0.5 s. Furthermore, (19) suggests that, for the residual Doppler shift not to exceed the 0.02% tolerance, $T_{\rm tp}$ should also be ~0.5 s (acceleration of ~1 m/s^2). For the purpose of simulation and experiment, a QPSK data block of 4096 symbols was used yielding a data rate of ~16 kbit/s. The simulation presented in the next section confirms the rationale of these statements.

B. Simulation Results

The results in this section are based on a simulated impulse response ($1 + 0.5z^{-2} + 0.3z^{-6}$) with additive white Gaussian noise (AWGN) to give an SNR of 15 dB. This corresponds to a multipath channel with a direct path and sea surface and bottom

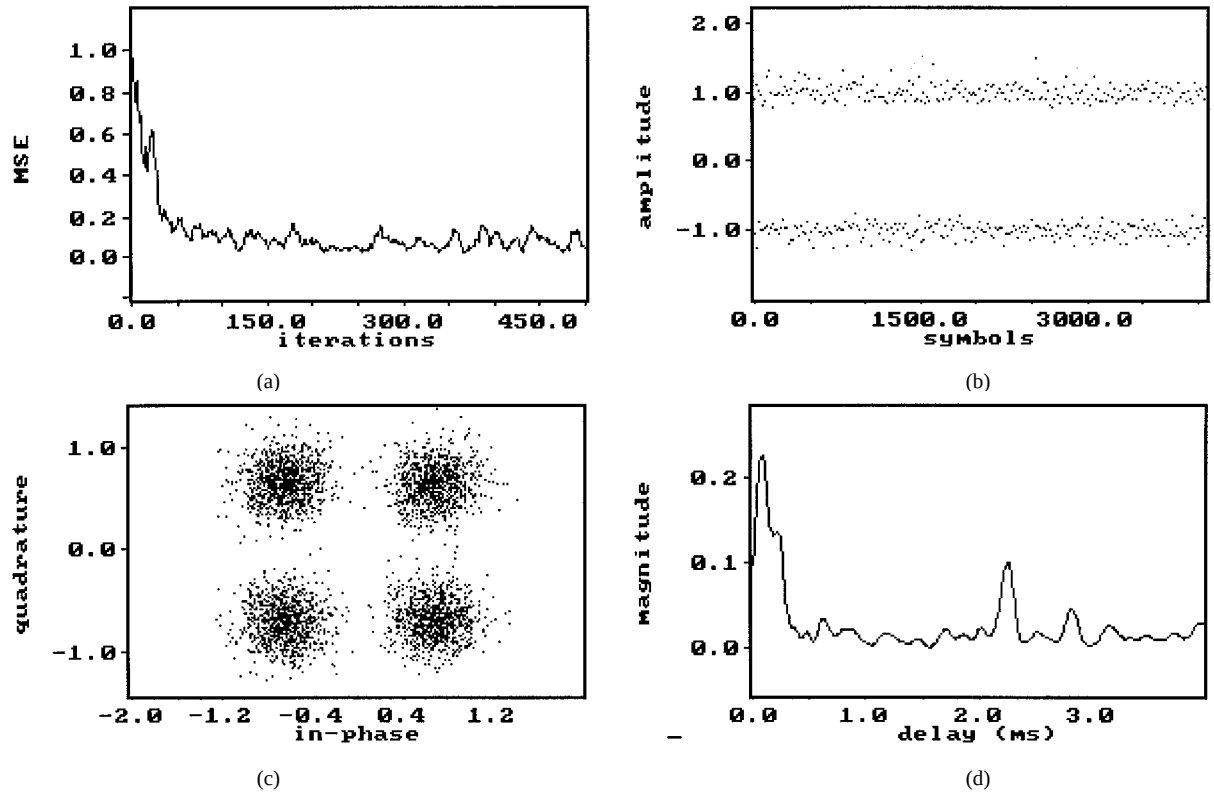

Fig. 11. Graphical output for +1.6-m/s velocity and 200-m range. (a) MSE curve during training. (b) Output envelope during data. (c) I–Q plot. (d) Channel impulse response.

reflections. Transmitter velocity and acceleration are simulated by interpolating the source signals by a constant or linearly ramped factor, respectively. The receiver structure, as shown in Fig. 7, consists of the Doppler preprocessor of Fig. 1, an in-phase-quadrature (I-Q) mixer, and a single-element DFE structure with 20 forward and feedback FIR taps (T/2 fractionally spaced) and LMS adaptation ($\mu = 0.001$) [8]. Fig. 8 shows a plot of the output SINR ($-10\log_{10}$(MSE)) of the adaptive receiver versus transmitter velocity, both with and without the Doppler preprocessor system. For zero velocity, both receivers achieve a satisfactory convergence with ~13-dB SINR, a level that would allow near error-free QPSK transmission. However, as the velocity increases, the MSE of the uncompensated receiver rapidly increases to an unacceptable level as the implicit synchronization of the equalizer fails. In fact, it requires a velocity of only ± 0.5 m/s to cause a significant increase in bit errors. In contrast, the figure shows that the receiver incorporating the Doppler preprocessor maintains near constant performance over the range of velocity of ± 6 m/s. It should be noted that a threshold could be used by the Doppler preprocessor, so that resampling is only performed if the estimated Doppler shift were above the level tolerated by the proceeding DFE structure (~10^{-4} for our application).

Fig. 9 shows the performance of the Doppler compensated receiver versus acceleration, with the starting velocity fixed at zero. There is only a small degradation (SINR drop of −1.5 dB) in receiver performance over the range of ± 3 m/s^2. If a nonzero starting velocity is chosen, then the performance curve is given by the superposition of Fig. 9 upon the corresponding velocity in Fig. 8. These simulation results verify that the design parameters chosen in (A) would meet the specification of $v = \pm 3$ m/s and α=±1 m/s^2.

C. Experimental Results

The Doppler estimation and compensation scheme presented in this paper was tested during experimental trials in the North Sea conducted in July 1998. Fig. 10 shows the experimental configuration used. The receiver structure was identical to that simulated above. However, in this case, a six-element rigid receiving array with λ spacing (15-kHz center frequency) was used followed by a bank of six tapped delay lines to form a wide-band adaptive beamformer [1]. The grating lobes effect resulting from λ spacing is circumvented by the directionality of the array transducers ($\pm 45^\circ$). In this case, Doppler estimation was performed on one element only, and the same value was used to compensate the signal from each element. This is a successful approach provided that array spacing is relatively small (~λ), otherwise separate estimation on each element may be required for large spatially-diverse arrays.

Figs. 11–14 show the output of the receiver system for various scenarios summarized in Table II. Each plot shows the convergence curve (MSE) during the training phase, the output envelope throughout the 4096-symbol, I-Q constellation and channel impulse response derived from the chirp correlation. In all cases, the velocity stated is from the Doppler estimator, which has a greater accuracy than the vessel's speed log. Fig. 11 shows a close range run with the transmitter moving toward the receiver, demonstrating error-free transmission (11.4-dB SINR). These

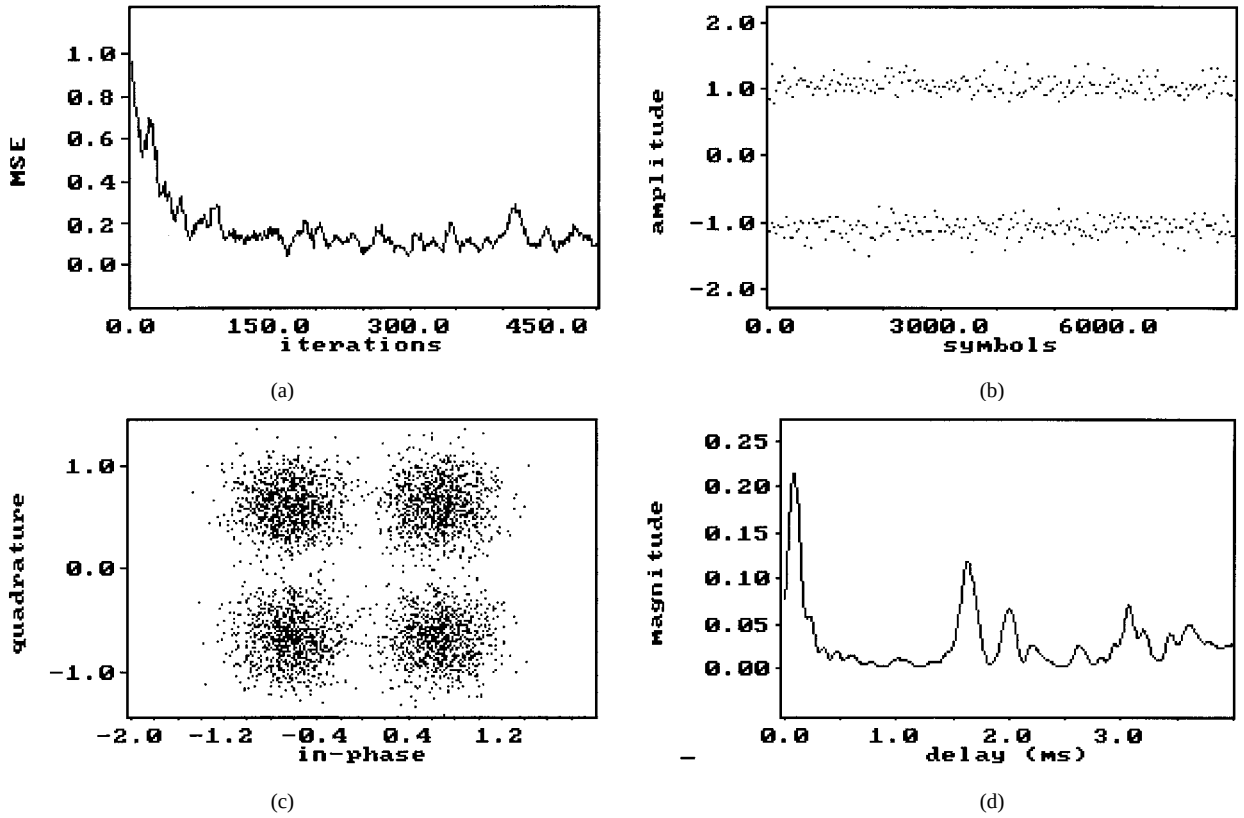

Fig. 12. Graphical output for −2.4-m/s velocity and 1000-m range. (a) MSE curve during training. (b) Output envelope during data. (c) I–Q plot. (d) Channel impulse response.

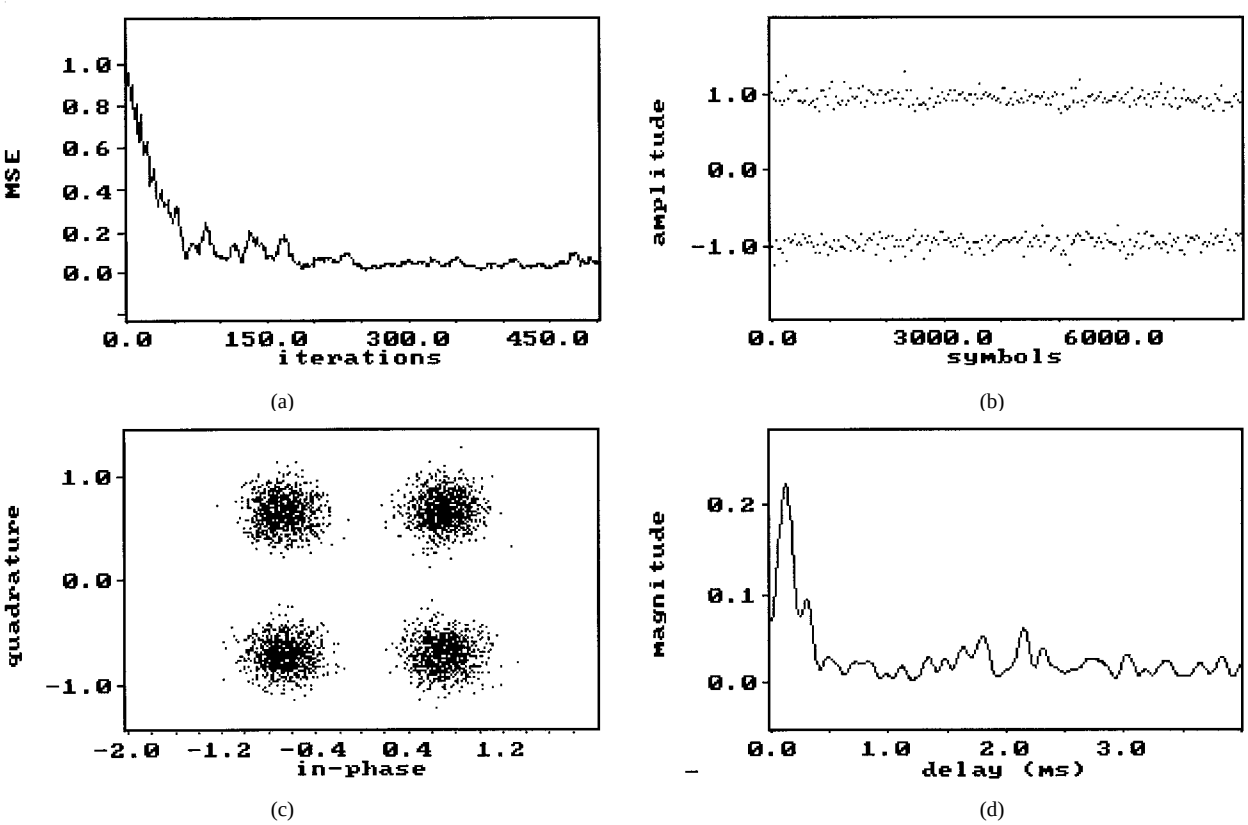

Fig. 13. Graphical output for −2.6-m/s velocity and 1700-m range. (a) MSE curve during training. (b) Output envelope during data. (c) I–Q plot. (d) Channel impulse response.

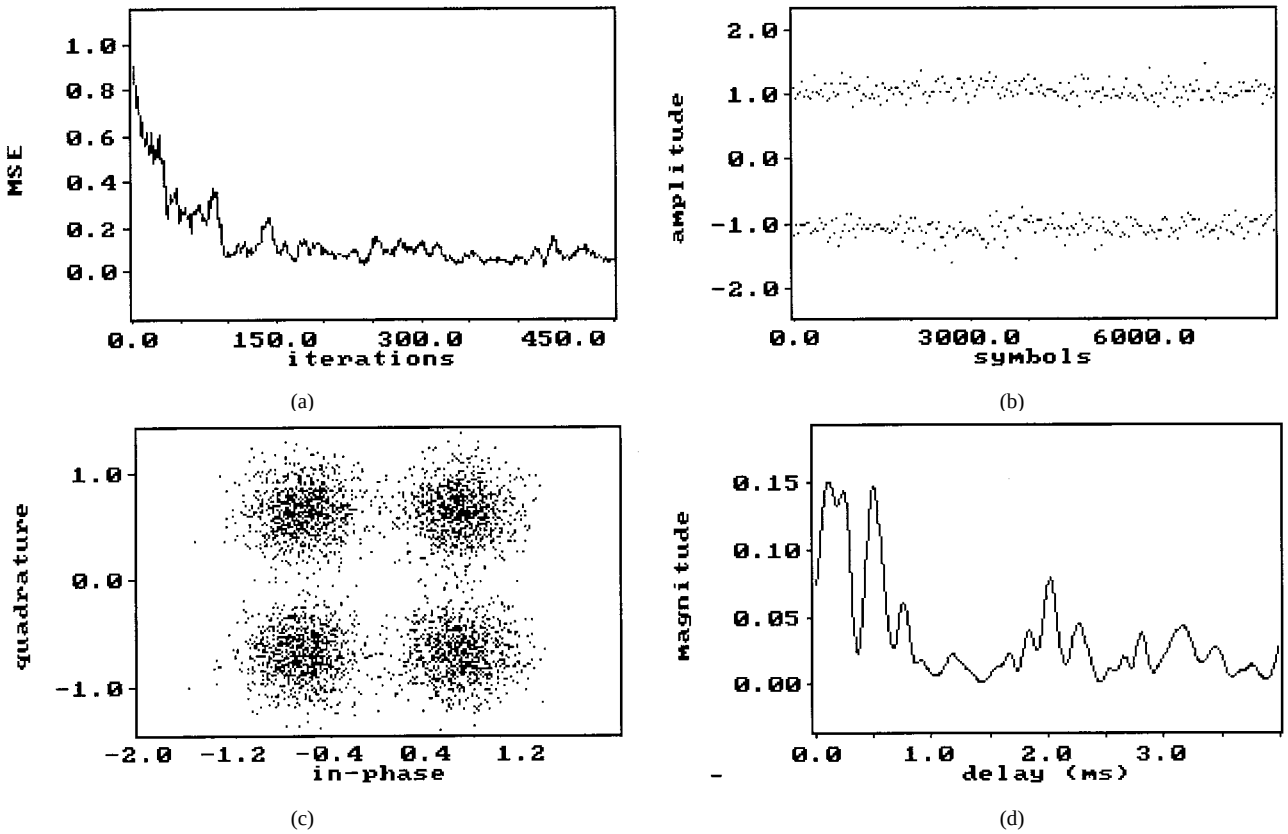

Fig. 14. Graphical output for –2.6-m/s velocity and 1900-m range. (a) MSE curve during training. (b) Output envelope during data. (c) I–Q plot. (d) Channel impulse response.

close range results along with the results shown in Figs. 12 and 14 are interesting because a significant Doppler spread or differential Doppler may be expected due to the angular separation of multipath. However, since the receiver is operating in a largely beamforming (spatial filtering) mode, then only the dominant direct-path Doppler must be precisely removed. This is demonstrated in the I-Q constellations where there is no evidence of phase rotation due to differential Doppler. The impact of multipath is more significantly related to the operational mode of the adaptive wide-band array structure, i.e., its temporal equalization versus beamforming resolution, for channels characterized by severe and widely varying multipath structure. This explains the improved performance obtained (13.5-dB SINR) in Fig. 13, where the multipath is relatively much smaller, when compared to the results obtained in Figs. 12 and 14 (9.5 and 9.9 dB, respectively), where strong multipath is evident. A receiver relying on purely temporal processing may well have to resolve the Doppler spread and compensate for differential Doppler resulting from individual paths.

In all cases, the performance of the communication system was comparable with that of a static transmitter for the same range, although exact channel conditions are impossible to reproduce. Despite the complex channel responses observed, the Doppler estimator proved to be very robust with false readings proving extremely rare. This supports the theory that sufficient channel stability is observed over short packets of 0.5 s. The output envelope plots, after equalizer training, clearly demonstrate that the Doppler estimation and interpolation process eliminates synchronization slippage. This result is supported by observing a complete synchronization failure upon removal of the Doppler preprocessor for tests involving moving platforms. Furthermore, even with a static transmitter, motion of the receiving vessel due to surface waves often gave rise to significant Doppler readings which would cause problems for the uncompensated receiver.

TABLE II
VARIOUS EXPERIMENTAL SEA TRIAL SCENARIOS

Range (m)	Velocity (m/s)	SINR (dB)	Errors in 8kbits
200	+1.6	11.4	0
1000	-2.4	9.5	19
1700	-2.6	13.5	0
1900	-2.6	9.9	23

Fig. 15 shows the variation in velocity over a period of 20 consecutive packets (9.4 s), for a short-range channel, with the bit error rate (BER) over the corresponding period. Despite the considerable variation in velocity (instantaneous acceleration up to 0.9 m/s^2 is observed), successful communication is achieved throughout the entire period with the BER in each 8192-bit (4096 symbols) data packet never exceeding 10^{-2}. In a total

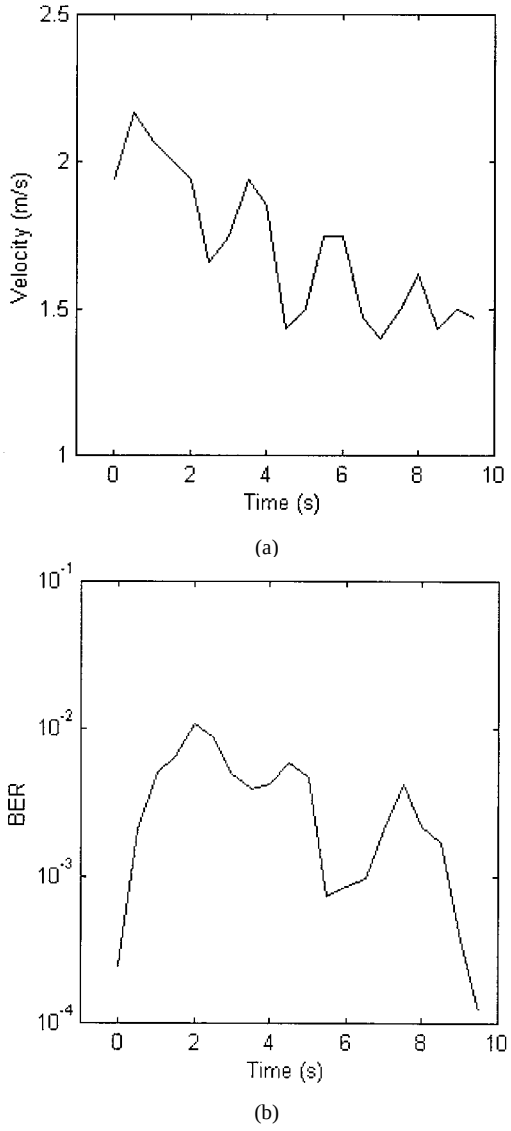

Fig. 15. (a) Estimated velocity and (b) measured BER over 9.4 s of continuous transmission (20 data packets). Range = 200 m.

of 20 kbit of data transferred in 9.4 s, there was only 589 bit errors (BER of ~3.6 * 10−3). Although our experimental facilities would not allow us to cover the full range of velocity and acceleration, the results presented are in agreement with the simulations presented earlier.

V. Conclusions

A Doppler-tolerant receiver has been demonstrated which is capable of communication at 16 kbit/s with a platform moving at up to 2.6 m/s with acceleration up to 0.9 m/s2. The data rate and range of velocities presented in this paper are constrained by the transducer specifications and the towing arrangements, respectively. However, this setup is representative of most AUV's deployed for commercial use. Furthermore, the results are in agreement with simulations which suggest that the system can cope with much higher velocity and acceleration should the need arise. In practice, it was often found that motion of the receiving vessel alone, due to surface waves, gave rise to Doppler effects, which would severely degrade the performance of an uncompensated receiver. A critical parameter in the system is the data packet length and, hence, how frequently we estimate Doppler and retrain the adaptive receiver. The packet length parameter influences the receiver's performance under platform acceleration, degree of sensitivity to channel variations, and ultimately accuracy of the Doppler estimates. In this application, a packet length of 0.5 s was found to satisfy the accuracy requirements while offering a high level of tolerance to acceleration and channel variations. However, the requirement for frequent Doppler estimation largely excludes this method from use with lower data rate systems where the bandwidth efficiency would fall dramatically. The low computational load of this receiver is its principle advantage. For the LFM chirp signal, only a single correlator with a relatively low BT product is required to estimate Doppler, the algorithm can be implemented using the same DSP hardware as an existing adaptive receiver [1]. Likewise, since simple linear interpolation at the receiver sampling rate (100 kHz) is employed for the Doppler compensation stage, the extra computations are of little significance. These factors should contribute to the development of a cost-effective solution for high-data-rate AUV telemetry in the near future.

References

[1] J. A. Neasham, D. Thompson, A. D. Tweedy, and O. R. Hinton, "Combined equalization and beamforming to achieve 20 kb/s acoustic telemetry for ROV's," in *Proc. IEEE Oceans '96*, Fort Lauderdale, FL, Oct. 1996, pp. 988–993.
[2] J. G. Proakis, *Digital Communications*, NY: McGraw-Hill, 1995.
[3] H. Meyr, "Synchronization in digital communications," in *Wiley Series in Telecommunications*. New York, NY: Wiley, 1990, vol. 1.
[4] A. W. Rihaczek, *Principles of High-Resolution Radar*: Peninsula Publishing, 1985.
[5] M. Johnson, L. Freitag, and M. Stojanovic, "Improved Doppler tracking and correction for underwater acoustic communications," in *Proc. ICASSP '97*, Munich, Germany, Apr. 1997, pp. 575–578.
[6] Z.-B. Lin, "Wideband ambiguity function of broadband signals," *J. Acoust. Soc. Amer.*, vol. 83, no. 6, June 1988.
[7] J. G. Proakis and D. G. Manolakis, *Digital Signal Processing—Principles, Algorithms and Applications*, 3rd ed. Englewood Cliffs, NJ: Prentice-Hall, 1996.
[8] M. Stojanovic, J. Catipovic, and J. Proakis, "Phase coherent digital communications for underwater acoustic channels," *IEEE J. Oceanic Eng.*, vol. 16, pp. 100–111, Jan. 1994.

Bayan S. Sharif (M'93) received the bachelor and doctorate degrees from Queen's University of Belfast and the Ulster University, Northern Ireland, in 1984 and 1988, respectively.

In 1989, he held a research fellowship post at Queen's University of Belfast, where he worked on parallel programming algorithms for image processing applications. He joined Newcastle University, Newcastle upon Tyne, U.K., in 1990 as a Lecturer in electronic engineering. He is currently a Senior Lecturer at Newcastle University, with research interests in digital signal processing algorithms for digital communications and image processing.

Dr. Sharif is a Chartered Engineer.

Jeff Neasham received the B.Eng. degree in electrical and electronic engineering from Newcastle University, Newcastle upon Tyne, U.K., in 1994.

He has since been working as a Research Associate in the Underwater Acoustic Group at the Department of Electrical and Electronic Engineering, Newcastle University. His research interests are mainly in the design and implementation of digital signal processing algorithms for underwater acoustic communications.

Oliver R. Hinton was born in 1947 in the U.K. He received the B.Sc.(Eng.) degree and the Ph.D. degree in microwave circuits from University College London, London, U.K., in 1968 and 1972, respectively.

After a lectureship in electronics at the University of Kent, he was appointed as Reader in microelectronics at Newcastle University, Newcastle upon Tyne, U.K., in 1987, and then in 1992, as Professor in Signal Processing. He has been a Visiting Scholar to Colorado State University and Stanford University. His research interests are in digital communications, image processing, and signal processing applications. He has published more than 80 papers in academic journals and conferences and has managed over 19 research contracts of a total value of over $1.5M. He was an invited Lecturer on the CEC Advanced Course on Acoustical Oceanography, invited delegate at the Regional Workshop of the UK Technology Foresight Programme, Cabinet Office of Science and Technology 1994, a UK Representative at the SERC/MTD N+N Meeting in Brighton in March 1994 on UK/US discussions for a joint Research Programme for Cleaner Seas.

Dr. Hinton serves on IEEE Professional Group Committee E5 and has been on the organizing committees of various conferences including the 3rd IEEE Conference on Telecommunications.

Alan E. Adams was born in Stoke-on-Trent, U.K., in 1949. He received the B.Sc. (Hons) degree in electronic engineering from the Polytechnic of North Staffordshire in 1970 and the M.Sc. degree from the University of Durham in 1977 for the development of a microprocessor based imaging system.

He is presently a Senior Lecturer with the Department of Electrical and Electronic Engineering at Newcastle University, Newcastle upon Tyne, U.K. He is the author of an undergraduate text on microprocessor systems. His current research interests center on the use of acoustic signals in the marine environment, for communication, imaging, and environmental measurements.

Mr. Adams is a member of the Institution of Electrical Engineers.